

## INVESTIGATION OF WAVE PROPAGATION IN A NONLINEAR DISPERSIVE TRANSMISSION LINE

Ali Ayhan TUNÇAY<sup>1</sup> ve Halil YARANERİ<sup>2</sup>

### Abstract

Nonlinear wave propagation in a nonlinear dispersive LC transmission line with linear inductance and nonlinear capacitance (varicap diode) is investigated. Dispersion in the line is introduced by second nearest neighbor interaction and controlled by reverse bias voltage. Waves at the region of group velocity dispersion are seen to be modulationally unstable and this leads to chaos with increase of wave amplitude. Emergence of chaos is investigated by Fourier and time-domain analyses, and via numerical simulations.

### Özet

Lineer bir bobin ve lineer olmayan bir kondansatörden (varikap diyot) oluşan lineer olmayan dağınımlı bir LC iletim hattındaki lineer olmayan dalga yayılımı incelendi. Hattaki dağınım, ikinci yakın komşu etkileşimi ile oluşturuldu ve diyota uygulanan ters öngerilim ile kontrol edildi. Grup hızı dağınımı bölgesindeki dalgaların modülasyona karşı kararsız olduğu ve bunun dalga genliğinin artmasıyla kaosa gittiği görüldü. Kaos'un ortaya çıkışı Fourier ve zaman bölgesi analizleri ve sayısal simülasyonlar yoluyla incelendi.

**Keywords:** *Wave propagation, nonlinear transmission line, modulational instability, chaos.*

### 1. Introduction

Nonlinear dispersive waves have attracted considerable attention both because of concept of integrability of partial differential equations for KdV, NLS and sine-Gordon equations and modulational instability of traveling waves which lead to creation of localized nonlinear excitations [1-3].

These two concepts, i.e., integrability and modulational instabilities are not independent but related through reductive perturbation method which is a way of deducing simplified equations from basic models [4]. The method is an asymptotic analysis of perturbation series in different scales. The scaling variables are determined via Taylor expansion of the frequency,  $\omega(k)$  with respect to deviation of wave number  $k$  due to nonlinearity [5].

In this work we will investigate evolution of wave in a discrete nonlinear lattice which has continuous time and discrete space variables by using reductive perturbation method for the discrete system.

Nonlinear lattice with finite next-nearest neighbor interaction is taken into account. Model system is applied to dispersive nonlinear LC transmission line.

---

<sup>1</sup> Adnan Menderes Üniversitesi, Aydın MYO, Teknik Programlar Bölümü, 09100 Merkez, Aydın

<sup>2</sup> Adnan Menderes Üniversitesi, Fen Edebiyat Fakültesi, Fizik Bölümü, 09100 Merkez, Aydın

## 2. Nonlinear LC transmission line

Transmission line considered in this work is shown in Figure 1. The line is composed of 130 identical sections and each one consists of a linear inductance  $L$ , linear capacitance  $C$  and a nonlinear capacitance  $C_N$ . In the experiment we use a varicap diode (Phillips BB112) with variable capacitance as nonlinear capacitance  $C_N$ . Capacitance is assumed to depend on voltage  $V = V_b + v_n$

$$C_N(V) = C_0 \left( 1 + \frac{V}{F} \right)^\kappa$$

where  $C_0$ ,  $F$  and  $\kappa$  are some characteristic parameters and  $V_b$  is the reverse bias voltage applied to the diode,  $v_n$  is the small signal voltage; for  $V=0$  we have  $C_N(0) = C_0$ .

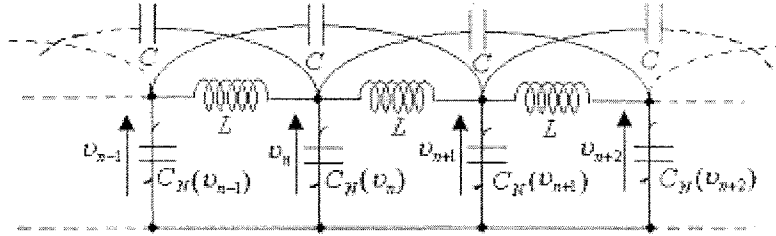


Figure 1. Nonlinear transmission line

The numerical values of line elements are  $C_0 = 2324$  pF,  $F = 0.75$  V,  $\kappa = -0.9$ ,  $C = 720$  pF,  $L = 1.78$   $\mu$ H,  $V_b = 2$  V, and corresponding  $C_{0b} = C(V_b) = C_0(1 + V_b / F)^\kappa = 721$  pF. The linear dispersion relation of the line is given as

$$\omega(k) = \frac{\omega_c \sin(k/2)}{[1 + \gamma \sin^2(k)]^{1/2}} \tag{1}$$

where  $\omega$  and  $k$  are angular frequency and wave number respectively,  $\gamma = \frac{4C}{C_{0b}}$  is a

dispersion factor and  $\omega_c = \frac{2}{\sqrt{LC_{0b}}}$  is the cutoff frequency [6].

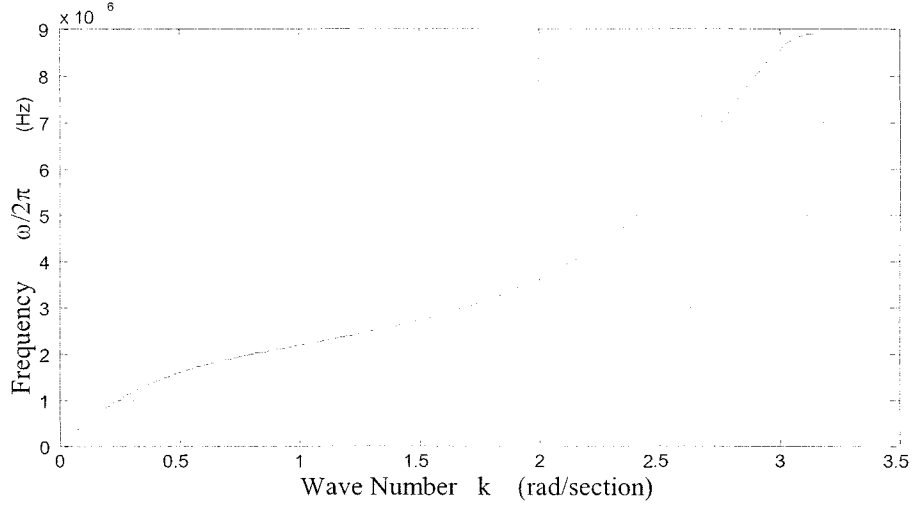


**Figure 2.** Dispersion relation of nonlinear transmission line

Dispersion relation of the line and voltage dependence of the  $C_N$  is given in Figure 2 and 3, respectively.

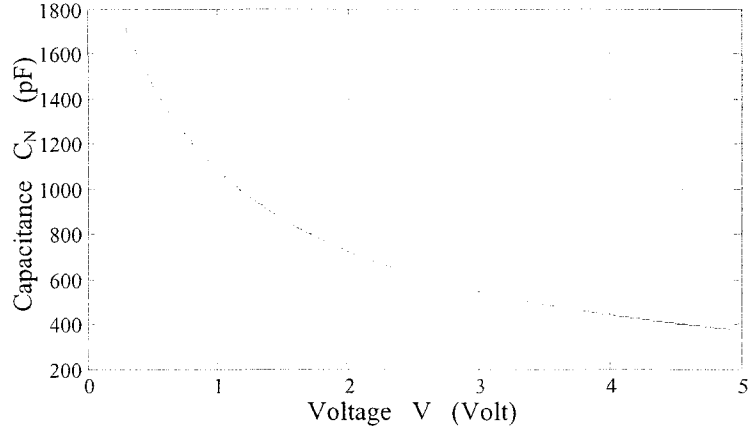


**Figure 3.** C-V graph of varicap diode

The equation of the transmission line, in the following differential-difference form, is

$$\frac{d^2 q_n}{dt^2} = C \frac{d^2}{dt^2} (v_{n+2} - 2v_n + v_{n-2}) + \frac{1}{L} (v_{n+1} - 2v_n + v_{n-1}) \quad (2)$$

$$\frac{dq_n}{dv_n} = C_N (V_b + v_n) = C_0 \left(1 + \frac{V_b + v_n}{F}\right)^\kappa \quad (3)$$

where  $q_n$  denotes charge stored in the nonlinear capacitance  $C_N(v_n)$ .

Expanding  $C_N(v_n)$  for small values of  $v_n$  Eq. (2) can be rewritten as

$$\frac{d^2 v_n}{dt^2} - (\gamma/4) \frac{d^2}{dt^2} (v_{n+2} - 2v_n + v_{n-2}) - V_{p0}^2 (v_{n+1} - 2v_n + v_{n-1}) = -\frac{d^2}{dt^2} (\mu v_n^2) \quad (4)$$

where  $\mu = \kappa/(2F)$ ,  $\gamma = 4C/C_{0b}$  and  $V_{p0} = 1/\sqrt{LC_{0b}}$  is phase velocity at the long wavelength limit.

### 3. Discrete multiple scale perturbation

We perform multi-scale analysis method on the discrete evolution Eq. (4). The problem is that of the propagation of a signal sent at the one end of the nonlinear transmission line (Figure 1). The method rely on the definition of a large grid scale via the comparison of the magnitude of the related difference operator and the on the expansion of the wave number in the powers of the frequency variations due to nonlinearity [7].

Considering the wave packet solution of the Eq. (4) as

$$v_n(t) = \int d\omega u(\omega) e^{i(kn-\omega t)} \tag{5}$$

one can expand the wave number  $k$  in terms of angular frequency  $\omega$  as

$$\omega = \Omega + \varepsilon v \tag{6}$$

$$k = K + \frac{\varepsilon v}{v_g} + \varepsilon^2 Q v^2 + \dots \tag{7}$$

where  $Q = \frac{1}{2} \left( \frac{\partial^2 K}{\partial \Omega^2} \right)$ . Solution of Eq. (4),  $v_n$ , can be defined as

$$v_n(t) = \varepsilon e^{i(Kn-\Omega t)} \phi(\xi, \tau) \tag{8}$$

with slow modulation  $\phi(\xi, \tau)$  is given as

$$\phi(\xi, \tau) = \int dv u(v) e^{i(\mu^2 Q \xi - v\tau)} \tag{9}$$

in the frame

$$\tau = \varepsilon \left( t - \frac{u}{v_g} \right), \quad \xi = \varepsilon^2 n \tag{10}$$

Long distance effect ( $\varepsilon^{-2}$ ) in the retarded time is considered in a way that input disturbance can have enough time to reach the observed point. Hence this corresponds to the situation where the lattice is excited at one end and its effect is detected at a point down the line.

Following the work of Leon and Manna [8] slow modulation  $\phi(\xi, \tau)$  of the plain wave  $A(n, t)$  will be represented by the function  $\phi(m, \tau)$  of the above defined discrete variable  $m$  and  $\tau = \tau_n$ . In the same way difference of  $v_n(t) = A(n, t) \phi(\xi, \tau)$  will be expressed as

$$\begin{aligned} v_{n+1} - 2v_n + v_{n-1} &= [A_{n+1} - 2A_n + A_{n-1}] \phi_m + \left( \frac{\varepsilon}{v_g} \right) [A_{n+1} - A_{n-1}] \partial_\tau \phi_m \\ &+ \left( \frac{\varepsilon}{v_g} \right)^2 \frac{1}{2} [A_{n+1} - A_{n-1}] \partial_\tau^2 \phi_m + \frac{\varepsilon^2}{2} [A_{n+1} - A_{n-1}] [\phi_{m+1} - \phi_{m-1}] \end{aligned} \tag{11}$$

and

$$\begin{aligned}
 v_{n+2} - 2v_n + v_{n-2} &= [A_{n+2} - 2A_n + A_{n-2}] \phi_m + \left( \frac{\varepsilon}{v_g} \right) [A_{n+2} - A_{n-2}] \partial_\tau \phi_m \\
 &+ \left( \frac{\varepsilon}{v_g} \right)^2 \frac{1}{2} [A_{n+2} - A_{n-2}] \partial_\tau^2 \phi_m + \frac{\varepsilon^2}{2} [A_{n+2} - A_{n-2}] [\phi_{m+1} - \phi_{m-1}]
 \end{aligned} \tag{12}$$

We will consider the onset of modulational instability and the effect of next nearest neighbor interactions on it in a nonlinear electrical lattice both experimentally and theoretically.

Equation of the line is given in Eq. (4).  $v_n$  is the voltage at the  $i^{\text{th}}$  cell. In the experiment signal is sent at the one end of the electrical lattice. Signal is slightly modulated plane wave for various values of the carrier frequency and amplitude. Output voltage is measured at the cell along the lattice.

A perturbation expansion of  $v_n$  is,

$$v_n = \sum_{p=1}^{\infty} \varepsilon^p \sum_{l=0}^p A^l(n, t) \phi_p^{(l)}(m, \tau) \tag{13}$$

where of course  $A^l(n, t) = \exp[i l(Kn - \Omega t)]$ .

Inserting the above expression in Eq. (4) and using the formula (11) and (12) we arrive the coefficients of the constant term gives at order  $\varepsilon$  :

$$\Omega^2 \phi_1^0 = 0 \tag{14}$$

at order  $\varepsilon^2$  :

$$\Omega^2 \phi_2^0 = 0 \tag{15}$$

at order  $\varepsilon^3$  :

$$\Omega^2 \phi_3^0 = 0 \tag{16}$$

from Eq. (14-16) it is seen that  $\phi_1^0 = 0$ ,  $\phi_2^0 = 0$ ,  $\phi_3^0 = 0$ .

The coefficients of  $A_n$  at order  $\varepsilon$  give

$$\phi_1^1 [-\Omega^2 (1 + \frac{\gamma}{2} - \frac{\gamma}{4} e^{-2ik} - \frac{\gamma}{4} e^{2ik}) + V_{p0}^2 (2 - e^{-ik} - e^{ik})] = 0 \tag{17}$$

which gives the dispersion relation (1). Then at order  $\varepsilon^2$  we obtain

$$\begin{aligned}
 &[-\Omega^2 (1 + \frac{\gamma}{2} - \frac{\gamma}{4} e^{-2ik} - \frac{\gamma}{4} e^{2ik}) + V_{p0}^2 (2 - e^{-ik} - e^{ik})] \phi_2^1 + \\
 &[-2i\Omega - \frac{1}{4v_g} \gamma \Omega^2 e^{-2ik} + \frac{1}{4v_g} \gamma \Omega^2 e^{2ik} + \frac{1}{v_g} V_{p0}^2 e^{-ik} - \frac{1}{v_g} V_{p0}^2 e^{ik}] (\phi_1^1)_\tau = 0
 \end{aligned} \tag{18}$$

The first line here vanishes due to the dispersion relation while the second one vanishes too thanks to

$$\Omega - \frac{1}{4v_g} \gamma \Omega^2 \sin 2k + \frac{1}{v_g} V_{p0}^2 \sin k = 0 \quad (19)$$

Finally the order  $\varepsilon$  with  $\phi_1^{(0)} = \phi_2^{(0)} = \phi_3^{(0)} = 0$  leads to

$$\begin{aligned} & [-\Omega^2 (1 + \frac{\gamma}{2} - \frac{\gamma}{4} e^{-2ik} - \frac{\gamma}{4} e^{2ik}) + V_{p0}^2 (2 - e^{-ik} - e^{ik})] \phi_3^1 + \\ & [-2i\Omega - \frac{1}{4v_g} \gamma \Omega^2 e^{-2ik} + \frac{1}{4v_g} \gamma \Omega^2 e^{2ik} + \frac{1}{v_g} V_{p0}^2 e^{-ik} - \frac{1}{v_g} V_{p0}^2 e^{ik}] (\phi_2^1)_\tau + \\ & [\frac{\csc k (\gamma \Omega^2 \cos 2k - 4V_{p0}^2 \cos k + (2 + \gamma - \gamma \cos 2k) v_g^2)}{2(\gamma \Omega^2 \cos k - 2V_{p0}^2) v_g^2}] (\phi_1^1)_{\tau\tau} - \end{aligned} \quad (20)$$

$$\begin{aligned} & [\frac{1}{2} \sin k (\gamma \Omega^2 \cos k - 2V_{p0}^2) (\Omega^2 (-2 - \gamma + \gamma \cos 4k) - 4(-1 + \cos 2k) V_{p0}^2)] |\phi_1^1|^2 \phi_1^1 + \\ & \frac{i}{2} [\phi_1^1 (m+1) - \phi_1^1 (m-1)] = 0 \end{aligned}$$

The first lines here vanish identically and we are left with the equation for  $\phi_1^1 = \eta$ ,

$$\frac{i}{2} [\eta_{m+1} - \eta_{m-1}] + Q \frac{\partial^2 \eta_m}{\partial \tau^2} - P |\eta_m|^2 \eta_m = 0 \quad (21)$$

with the following K-dependent coefficients

$$Q = \frac{\csc K (\gamma \Omega^2 \cos 2K - 4V_{p0}^2 \cos K + (2 + \gamma - \gamma \cos 2K) v_g^2)}{2(\gamma \Omega^2 \cos K - 2V_{p0}^2) v_g^2} \quad (22)$$

And

$$P = \frac{1}{2} \sin K (\gamma \Omega^2 \cos K - 2V_{p0}^2) [\Omega^2 (-2 - \gamma + \gamma \cos 4K) - 4(-1 + \cos 2K) V_{p0}^2] \quad (23)$$

The continuous version of the Eq. (21) is a well known model for boundary value problems in optical fibers [9]. It has been investigated also in the case of initial value problems in unstable media [10] to describe for instance Rayleigh-Taylor instability.

The plane wave solution to Eq.(21),

$$\eta_m(\tau) = B \exp[i(\lambda m - \nu \tau)] \quad (24)$$

obeys the dispersion relation

$$\nu^2 = -\frac{1}{Q} [\sin \lambda + P |B|^2] \quad (25)$$

As we are considering a boundary value problem,  $\nu$  and  $B$  are frequency and amplitude of the modulation, respectively. Then, as  $\sin \lambda$  is bounded there is no real solution for  $\lambda$  if,

$$Q > 0, \quad |B^2| > \frac{1}{P} = B_{cr}^2 \quad (26)$$

This is a discreteness effect and it leads to unstable plane waves.

Taking Eq. (22) and Figure 4 into consideration we remark that  $Q$  vanishes at  $K = K_{cr}$ . For these values of  $K$  the group velocity of dispersion becomes zero. To investigate the effect of next neighbor interaction  $\gamma$  on the modulational instability, we calculated  $Q(K)$  for  $\gamma = 0.05, 1.05, 2.05, 3.05, 4.05, 5.05$  and plotted the result in Figure 4.

It is easily seen at Figure 4 that  $Q(K)$  graph shoots around  $K = 0.2$  and also is not very sensitive to the value of  $\gamma$  at that range. It seems that for  $\gamma > 0$  low frequency (envelope) becomes unstable. Increase in the value of  $\gamma$  increases the instability of waves around  $K = 0.75$ . Steep increase in the value of  $Q(K)$  at  $K = 0.2$  compared to the maximum at  $K = 0.75$  indicates that former is more dominant than the latter.

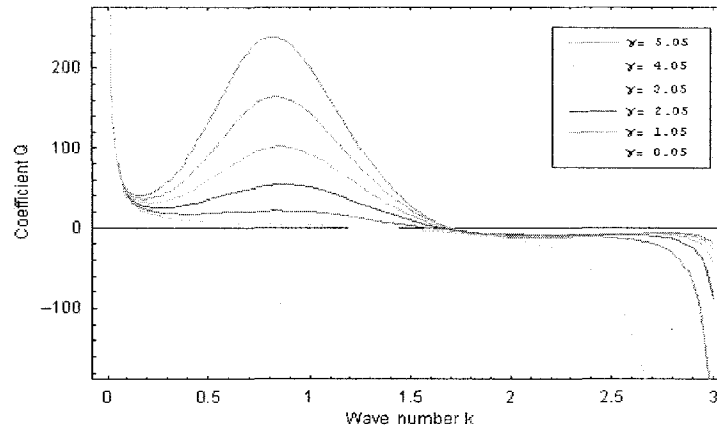
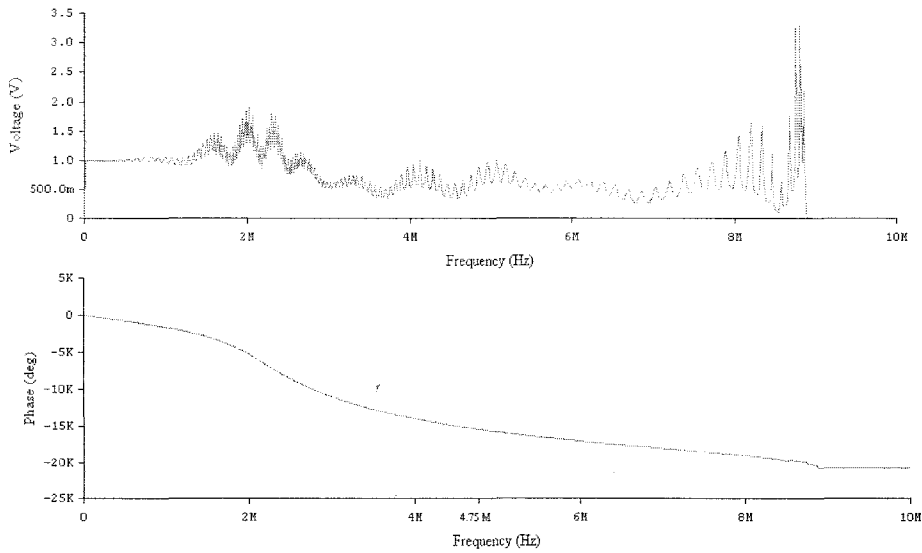


Figure 4. Graph of coefficient  $Q$  for the different values of  $\gamma$

#### 4. Computer Simulations

In numerical experiments using Electronics Workbench (EWB v5.12) software, we tried to see modulational instability by sending an Amplitude Modulated (AM) signal which is modulated by a sinusoidal wave from the beginning of nonlinear transmission line described in Section 2. Modulation index of the AM signal is chosen to be 1. Carrier frequency is selected to be a resonance frequency at 4750 kHz, where the group velocity of short wave (carrier) equals the phase velocity of the long waves, as shown in Figure 5. The modulating frequency is selected to be 500 kHz which needs to be small enough to stay within the relatively linear region of the amplitude response



**Figure 5.** Frequency response of the line and selection of carrier frequency used in the simulations.

The frequencies used in this experiment are specifically chosen using the dispersion curve to make resonant interaction possible.

The transient analysis of the signals with their Fourier Transforms down the line at the 120<sup>th</sup> cell for the carrier amplitude of  $V_c = 50$  mV, 100 mV, 200 mV, 400 mV, and 800 mV is given in Figures 6-9<sup>1</sup>. Results clearly show that with the increase in the amplitude of carrier wave more and more energy is transferred to low frequency modes ( $K = 0.2$ ) and it makes envelope wave unstable, in other words modulated wave starts to be re-modulated as it is shown in the figures. With the further increase in the amplitude of  $V_c$  energy is transferred to  $K = 0.75$  modes as well and finally as more and more modes excited system goes in to chaotic state.

Experimental measurements are quite in line with the theoretical calculations. Main instability of the system is in  $K = 0.2$  linear region of dispersion curve. This corresponds to low frequency instability and energy is transferred to low frequency modes in Benjamin-Feir sense [11]. Other unstable region around  $K = 0.75$  does not play significant role for  $V_c < 500$  mV, however, for  $V_c > 500$  mV it participates in exciting other modes and system becomes chaotic (Figure 9).

<sup>1</sup> Note that, because of a bug in the EWB software, one needs to use the square-root of the desired carrier amplitude value when setting the “AM Source” properties. For example, to get 50 mV, use 223.6 mV.



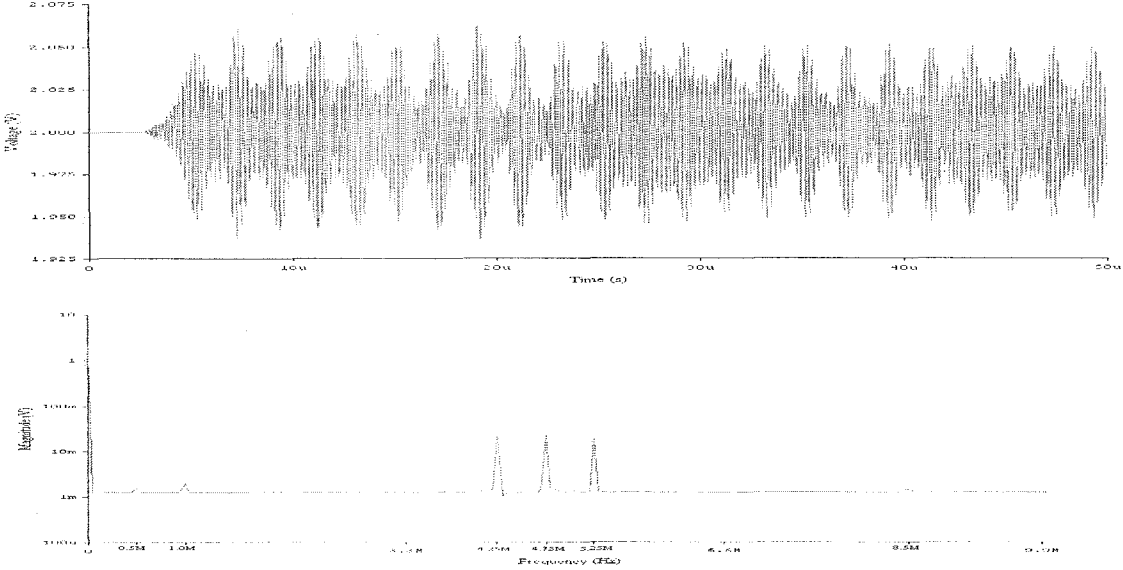


Figure 6. Observed waveform and its spectrum at  $n = 120, V_c = 50 \text{ Mv}$

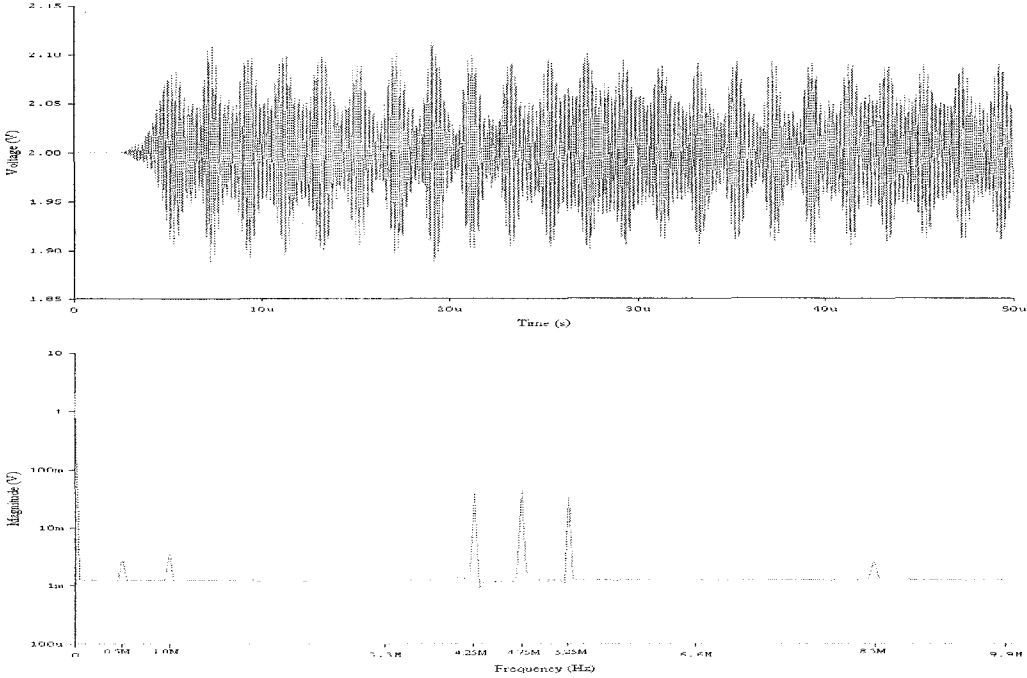


Figure 7. Observed waveform and its spectrum at  $n = 120, V_c = 100 \text{ mV}$

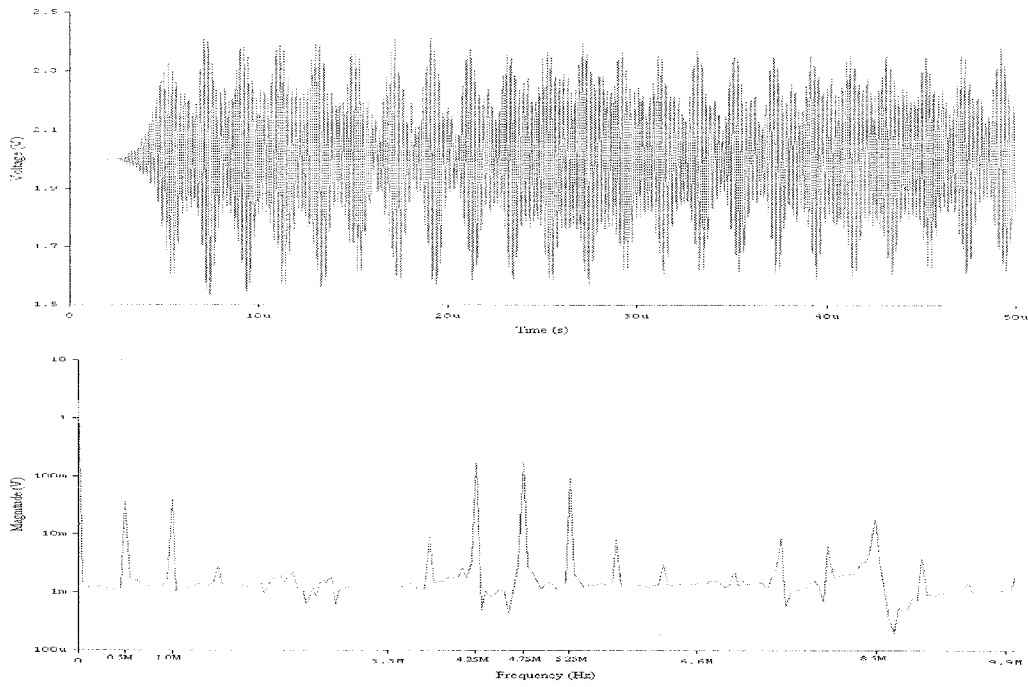


Figure 8. Observed waveform and its spectrum at  $n = 120$ ,  $V_c = 400$  mV

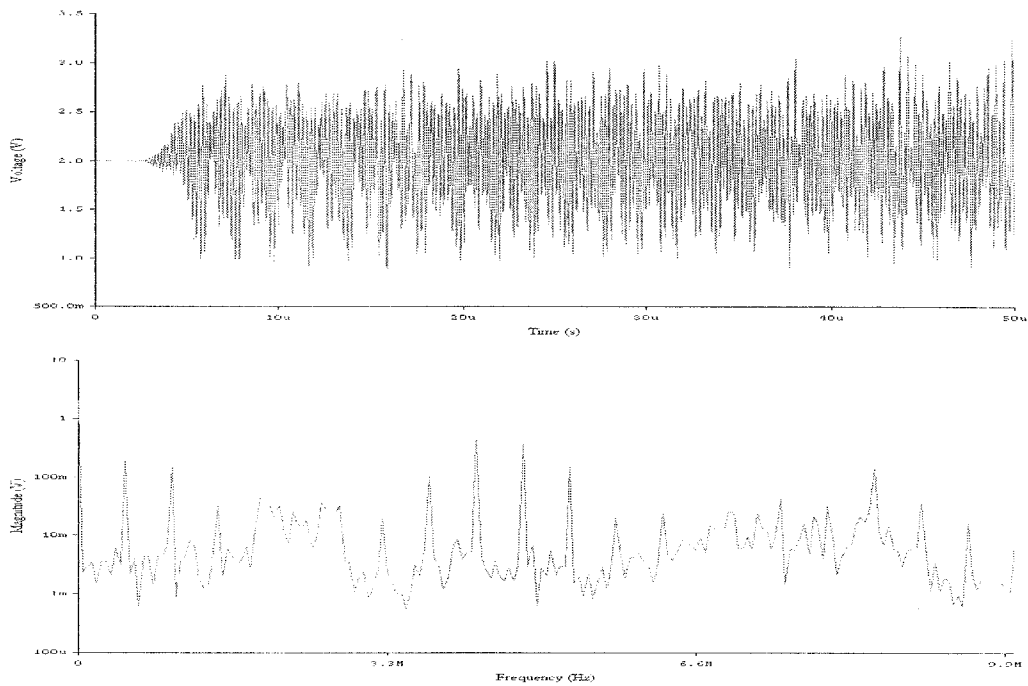


Figure 9. Observed waveform and its spectrum at  $n = 120$ ,  $V_c = 800$  mV

To investigate instability and chaotic nature of the system we also plot transient outputs of adjacent points as XY graph for  $V_c = 50\text{-}800$  mV (Figure 10). These resemble the phase space graph of dynamical systems. It is seen from the graph that as  $V_c$  increases system cover the more and more phase plane space and this indicates the presence of chaotic like behavior of the system. For more precise results we are planning to calculate Lypunov exponent of the system.

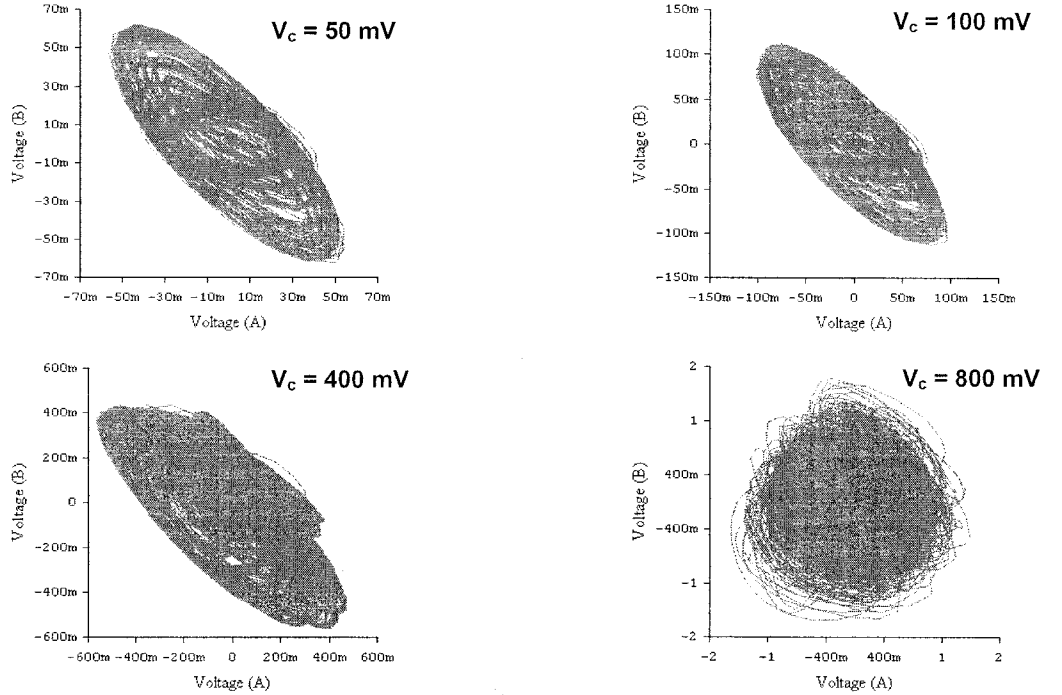


Figure 10. Phase-space plots ( $V_{121}$  vs  $V_{122}$  plots) for 250  $\mu$ s of simulation

#### 4. Conclusions

The instability described in this work results from wave scattering in a nonlinear medium (boundary value problem) which requires to use a change of variables like Eq. (10) which in turn leads to the unstable wave equation (21) for the envelope. The resulting instability is for *boundary value problem* then of first order and has the similar universal character as the Benjamin-Feir instability for initial value problems [11, 12]. This instability is a purely discrete phenomenon.

We performed a semi-discrete (discrete carrier and continuous envelope) analysis with the new variables Eq. (10) and get to the dispersion law

$$\nu^2 = -\frac{1}{Q}[\sin \lambda + P|B^2|] \quad (30)$$

For positive values of  $Q$ , there is no real solution  $\lambda$  of above dispersion relation for any given modulation frequency  $\nu$  which leads to modulational instability in the system. This is

also confirmed by computer simulations of the nonlinear transmission line. Both our calculations and experiments show that magnitude of second nearest neighbor interaction enhances the modulational instability in the system.

We found two instability region at around  $K = 0.2$  and other around  $K = 0.75$ . The second one is found to be quite insignificant compared to first one. Instability at  $K = 0.2$  is Benjamin-Feir type instability and the one at  $K = 0.75$  participates in driving system to chaotic like regime.

Instability depends on the input wave amplitudes. This implies that due to wave-wave resonance interaction in the line, above certain amplitude threshold, energy of high frequency waves starts to transfer to low frequency waves, and modulated wave amplitude increases. This enhances the effect of nonlinearity in the line and causes new frequencies to appear, leading to chaotic behavior.

### References

- [1] Gardner, C.S., Gren, J.M., Kruskal, M.D., Miura, R.M., (1967), *Phys. Rev. Lett.*, 19, 1095.
- [2] Zakharov, V.E., Shabat, A.B., (1972), *Sov. Phys. JETP*, 34, 62. [(1971), *Zh. Eksp. Teor. Fiz.*, 6, 118.]
- [3] Ablowitz, M.J., Kaup, D.J., Newell, A.C., Segur, H., (1974), *Stud. Appl. Math.*, 53, 249.
- [4] Leon, J., Manna, M., (1999), *J. Phys. A: Math. Gen.*, 32, 927-943.
- [5] Nayfeh, A.H., (1993), *Introduction to Perturbation Techniques*, New York, Wiley.
- [6] Yoshinaga, T., Yamamoto, T., Kakutani, T., (1989), *Nonlinear Wave Motion* (Ed. Alan Jeffrey), Pitman, Longman Group, Essex, 229-245.
- [7] Leon, J., Manna, M., (1999), *J. Phys. A: Math. Gen.*, 32, 2845.
- [8] Leon, J., Manna, M., (1999), *Phys. Rev. Lett.*, 83, 2324.
- [9] Hasegawa, A., Tappert, F., (1974), *Appl. Phys. Lett.*, 23, 284.
- [10] Wadati, M., Iizuka, T., Yajima, (1991), *Physica D*, 51, 388.
- [11] Benjamin, T.B., Feir, J.E., (1967), *Fluid Mech.*, 27, 417.
- [12] Bespalov, V.I., Talanov, V.I., (1966), *Sov. Phys. JETP Lett.*, 3, 307. [(1966), *Pis'ma Zh. Exp. Teor. Fiz.*, 3, 471.]